Enhancement of multifiber beam elements for RC structures with lateral confinement due to stirrups

Natalia Khoder[1], Stéphane Grange[2], Yannick Sieffert[3]

[1] PhD student, Univ Lyon, INSA-LYON, GEOMAS, F-69621, Villeurbanne, France.
[2] Professor, Univ Lyon, INSA-LYON, GEOMAS, F-69621, Villeurbanne, France.
[3] Associate Professor, Univ. Grenoble Alpes, CNRS, Grenoble INP, 3SR, 38000 Grenoble, France

ABSTRACT

Many researches have been conducted in the structural engineering field in order to develop efficient numerical tools able to reproduce the complex nonlinear behavior of reinforced concrete structures. In the case of slender elements, enhanced beam models have been developed to try to introduce shear effects, but in these models, the transverse steel is sometimes taken into consideration with approximated manner or often not at all. However, as shown by some experimental tests, the amount of transverse reinforcement triggers significantly the behavior of beam elements, especially under cyclic loading. The present study addresses this problem by investigating solutions for an enhanced multifiber beam element, accounting for transversal stretching of the cross-section occurring due to the presence of stirrups. A Timoshenko beam element with internal degrees of freedom and higher order interpolation functions is selected. Full 3D stresses and strains are obtained and the construction of the element and sectional stiffness matrices is detailed. The element presented hereafter is suitable for an arbitrary shape cross-section made of heterogeneous materials. Numerical applications considering linear elastic and non-linear behavior of the materials are performed and compared to experimental results.

Keywords: Multifiber beam, Confinement, Stirrups, Reinforced concrete, Cyclic loading.

INTRODUCTION

To study the seismic vulnerability of existing reinforced concrete structures, numerical computations at the structural scale able to account for material nonlinearities are needed. 2D and 3D finite element formulations are too costly, whereas multifiber beam elements combine the advantages of high computational speed with an increased accuracy for nonlinear materials. The principle of multifiber modeling consists on adding a two dimensional section at the Gauss point of the element. Each section is afterwards discretized into several elements presenting Gauss points where stresses and strains are computed. To this end, generalized strains are obtained at the beam Gauss points from the node displacements. Then, based upon Euler-Bernoulli or Timoshenko's theory, they are used to calculate the total strains, and with an adequate constitutive law, stresses are deduced at the Gauss points of the section. The generalized forces are finally derived after integration made over the cross-section [1].

A variety of approaches have been developed to try to introduce shear effects, such as those proposed by [2], but whose model can't be applied to reinforced concrete elements, and the numerical formulation of [3] which is adapted to reinforced concrete applications but works only in 2D. More recently, [4] developed a nonlinear multifiber beam model which provides robust results by the introduction of torsional warping in the case of reinforced concrete beams subjected to shear dominating loads.

In the above-mentioned works, the transverse steel is sometimes taken into consideration with approximated manner or often not at all. However, as shown by some experimental tests conducted by [5], the amount of transverse reinforcement triggers significantly the behavior of beam elements, especially under cyclic loading.

Hereafter, a 3D enhanced multifiber beam model able to account for the distortion of the section is presented. It's a displacement-based formulation and higher order interpolation functions are involved in order to avoid shear-locking problems. Moreover, longitudinal and transversal rebars are introduced in the numerical model and their implementation is validated by comparisons performed with numerical and experimental results in the non-linear domain.

PROPOSED MODEL

Section Kinematics

A 3D multifiber Timoshenko beam, displacement-based, element has been developed. The main assumption considered herein is that the full displacement of any fiber at the cross-section level is defined by the superposition of the traditional rigid body displacements of the plane section ($\mathbf{u^P}$) obtained with Timoshenko's theory, plus an additional displacement field ($\mathbf{u^w}$) (like in [6]). The latter one has two transversal components, u_y^w and u_z^w, which stand for the distortion of the section in y and z directions respectively. The total displacement (u) of any fiber is given by the following equation:

$$\mathbf{u} = \underbrace{\begin{bmatrix} U_x(x) - y\theta_z(x) + z\theta_y(x) \\ U_y(x) - z\theta_x(x) \\ U_z(x) + y\theta_x(x) \end{bmatrix}}_{\boldsymbol{u^P}} + \underbrace{\begin{bmatrix} 0 \\ u_y^w(x,y,z) \\ u_z^w(x,y,z) \end{bmatrix}}_{\boldsymbol{u^w}} \tag{1}$$

U_x, U_y and U_z being the translations in x, y and z directions respectively. As for θ_x , θ_y and θ_z , they denote the three rotations about x, y and z axes respectively, for a standard 3D beam element.

Under the assumption of small displacements, the total strain at any point will be formed by the sum of the plane strain field ($\boldsymbol{\varepsilon^P}$) and the distortional strain ($\boldsymbol{\varepsilon^w}$) as follows:

$$\boldsymbol{\epsilon} = \frac{1}{2}\left(grad(\boldsymbol{u}) + grad(\boldsymbol{u})\right)^T = \boldsymbol{\epsilon^P}(\boldsymbol{u^P}) + \boldsymbol{\epsilon^w}(\boldsymbol{u^w}) \tag{2}$$

Therefore, the 6 components of the total strain field are defined as follows expressed in function of the generalized deformation vector $\mathbf{e_s}$, and a compatibility matrix $\mathbf{a_s}$(y,z) so that $\boldsymbol{\varepsilon^P}$ takes the following form:

$$\boldsymbol{\epsilon^P} = \underbrace{\begin{bmatrix} 1 & 0 & 0 & 0 & +z & -y \\ 0 & 0 & 0 & 0 & 0 & 0 \\ 0 & 0 & 0 & 0 & 0 & 0 \\ 0 & 1 & 0 & -z & 0 & 0 \\ 0 & 0 & 1 & y & 0 & 0 \\ 0 & 0 & 0 & 0 & 0 & 0 \end{bmatrix}}_{\boldsymbol{a_s}(y,z)} \underbrace{\begin{bmatrix} \frac{dU_x}{dx} \\ \frac{dU_y}{dx} - \theta_z \\ \frac{dU_z}{dx} + \theta_y \\ \frac{d\theta_x}{dx} \\ \frac{d\theta_y}{dx} \\ \frac{d\theta_z}{dx} \end{bmatrix}}_{\boldsymbol{e_s}} \tag{3}$$

Also, as can be seen from equation (1), the distortional displacement (u^w) will contribute to the lateral deformation components (ε_{yy}) and (ε_{zz}). Therefore, transverse strains are not null, and the additional strains ($\boldsymbol{\varepsilon^w}$) play an important role in the description of the vertical stretching of the section. As a consequence, the effect of transversal reinforcement described by lateral expansion and contraction, can be taken into account. Hence, the behavior of confined reinforced concrete elements can be studied.

Caillerie's Timoshenko beam element with internal degrees of freedom

In order to avoid shear locking problems coming from the use of linear interpolation functions, several authors [6-7] have developed numerical models based on higher order interpolation functions or functions depending on material properties. However, the latter ones present the disadvantage of not being updated after damage. Recently, a new multifiber beam element has been developed by [8] and has been chosen to be used. It is presented by Figure 1.

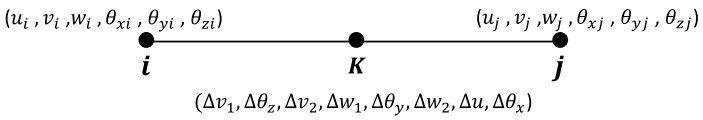

Figure 1. Definition of the degrees of freedom in the 3D version of Caillerie's beam element

Each of the two nodes (i and j) has 6 degrees of freedom: 3 translations (u, v, w) and 3 rotations (θ_x , θ_y , θ_z) about x, y and z axes respectively. The proposed element was developed by [8] for 2D applications and was extended in our model to a 3D formulation and enhanced by [9] in order to avoid normal force/bending moment locking. Therefore, it presents an internal node K, with 9 internal degrees of freedom (Δv_1,Δv_2,Δw_1,Δw_2,$\Delta\theta x$,$\Delta\theta y$,$\Delta\theta z$ and Δu_1 and Δu_2). The generalized displacement

field can be interpolated using quadratic and cubic functions (see [8]). As a consequence, the generalized strain field $\mathbf{e_s}$ can be written in function of a matrix $\mathbf{B_p}$, which gathers the derivatives of the above, mentioned interpolation functions related to longitudinal spatial discretization. Then, the new expression of the plane strain field $\boldsymbol{\varepsilon}^{\mathbf{P}}$ becomes:

$$\boldsymbol{\epsilon}^{\boldsymbol{P}} = \boldsymbol{a_s}(y,z)\boldsymbol{B_p}\boldsymbol{U}^{\boldsymbol{e}} \tag{4}$$

Distortional displacement field interpolation

It is assumed that the distortional displacement (u^w) has two non-zero components in y and z directions accounting for the vertical stretching of the cross-section. It is defined as:

$$\boldsymbol{u}^{\boldsymbol{w}}(x,y,z) = \begin{bmatrix} 0 & u_y^w(x,y,z) & u_z^w(x,y,z) \end{bmatrix} \tag{5}$$

Where:

$$\begin{cases} u_x^w(x,y,z) &= 0 \\ u_y^w(x,y,z) &= c_1(x)\varphi_1(y,z) \\ u_z^w(x,y,z) &= c_2(x)\varphi_2(y,z) \end{cases} \tag{6}$$

As in [2], the interpolation is performed independently along the beam axis with the quadratic functions $c_1(x)$ and $c_2(x)$, and on the cross-section with functions $\varphi_1(y,z)$ and $\varphi_2(y,z)$. The latter ones are the classical quadratic functions used for 6 nodes triangular elements TRI6 and they are computed at the section Gauss points. Enhanced distortional strains components can be therefore presented as follows:

$$\boldsymbol{\epsilon}^{\boldsymbol{w}} = \begin{bmatrix} \epsilon_{xx}^w \\ \epsilon_{yy}^w \\ \epsilon_{zz}^w \\ \gamma_{xy}^w \\ \gamma_{xz}^w \\ \gamma_{yz}^w \end{bmatrix} = \underbrace{\begin{bmatrix} 0 & 0 & 0 & 0 \\ 0 & 0 & \frac{\partial \varphi_1}{\partial y} & 0 \\ 0 & 0 & 0 & \frac{\partial \varphi_2}{\partial z} \\ \varphi_1 & 0 & 0 & 0 \\ 0 & \varphi_2 & 0 & 0 \\ 0 & 0 & \frac{\partial \varphi_1}{\partial z} & \frac{\partial \varphi_2}{\partial y} \end{bmatrix}}_{\boldsymbol{a_w}(y,z)} \underbrace{\begin{bmatrix} \frac{dc_1}{dx} \\ \frac{dc_2}{dx} \\ c_1 \\ c_2 \end{bmatrix}}_{\boldsymbol{e_w}} \tag{7}$$

Then the vector $\mathbf{e_w}$ can be written using a matrix $\mathbf{B_w}$ collecting the longitudinal interpolation functions and their derivatives, and a vector $\mathbf{W_e}$ gathering all the distortional degrees of freedom of the points located on the section i of each element (see equation 8 for the details of the components). They are treated as global DOFs of the beam element as shown by Figure 2 but they also can be statically condensed in the global degrees of freedom (in the way of the E-FEM).

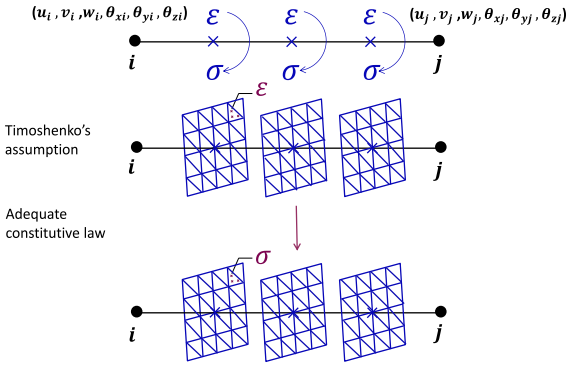

Figure 2. Calculation procedure

With the enhancement components:

$$\begin{aligned} \boldsymbol{W}^e_{y(i,j)} &= \begin{bmatrix} u^w_{y1(i,j)} & \dots & u^w_{ynw(i,j)} \end{bmatrix}^T \\ \boldsymbol{W}^e_{z(i,j)} &= \begin{bmatrix} u^w_{z1(i,j)} & \dots & u^w_{znw(i,j)} \end{bmatrix}^T \\ \Delta\boldsymbol{W}_{(y,z)} &= \begin{bmatrix} \Delta u^w_{(y,z)1} & \dots & \Delta u^w_{(y,z)nw} \end{bmatrix}^T \end{aligned} \tag{8}$$

n_w being the total number of the nodes per section. Once the plane strain $\boldsymbol{\varepsilon}^{\mathbf{P}}$ and the distortional strain fields $\boldsymbol{\varepsilon}^{\mathbf{w}}$ computed at the Gauss points of the section, the stress distribution at the concrete fibers is deduced. 3 Gauss points per element are needed in order to correctly integrate the higher order polynoms, which means 3 sections per element. Thus, Figure 2 can illustrate the calculation procedure.

GOVERNING EQUATIONS

Beam equilibrium is written in its weak form by equation (9). In addition, the plane section displacement $\mathbf{u}^{\mathbf{P}}$ and the distortion one u_w assumed to be orthogonal (by a projection of the interpolation function in the way initially proposed by [2]), the projection of the weak form equilibrium on these two subspaces lead to two equilibrium equations (9). The first one representing the classical equilibrium of the beam element, and the second one being the equilibrium equation of the cross-section. $\mathbf{F}$ denotes the external forces and $\mathbf{P}^{\mathbf{w}}$ the forces coming from constrained distortion at the beam ends.

$$\int_{\Omega} \boldsymbol{\epsilon}^{*T} \boldsymbol{\sigma} d\Omega = \boldsymbol{U}^{*T} \boldsymbol{F_{ext}} \Leftrightarrow \begin{cases} \int_{\Omega} \delta \boldsymbol{\epsilon}^{\boldsymbol{P}^T} \hat{\boldsymbol{\sigma}}(\epsilon^P, \epsilon^w) d\Omega & = \boldsymbol{F} \\ \int_{\Omega} \delta \boldsymbol{\epsilon}^{\boldsymbol{w}^T} \hat{\boldsymbol{\sigma}}(\epsilon^P, \epsilon^w) d\Omega & = \boldsymbol{P^w} \end{cases} \tag{9}$$

At the element level, the beam is discretized into n_e Timoshenko beam elements, of length l_e, each having 3 Gauss points, i.e. 3 sections, whose contribution should be summed in order to compute the terms of the element force vector $\mathbf{P_e}$ and the element stiffness matrix $\mathbf{K_e}$.

$$\boldsymbol{K_e} = \begin{bmatrix} \boldsymbol{K_{pp}} & \boldsymbol{K_{pw}} \\ \boldsymbol{K_{wp}} & \boldsymbol{K_{ww}} \end{bmatrix} \quad \begin{aligned} \boldsymbol{K_{pp}} &= \int_{l_e} \boldsymbol{B_p}^T \boldsymbol{a_s}^T \boldsymbol{K_m} \boldsymbol{a_s} \boldsymbol{B_p} dx \\ \boldsymbol{K_{pw}} &= \int_{l_e} \boldsymbol{B_p}^T \boldsymbol{a_s}^T \boldsymbol{K_m} \boldsymbol{a_w} \boldsymbol{B_w} dx \\ \boldsymbol{K_{wp}} &= \int_{l_e} \boldsymbol{B_w}^T \boldsymbol{a_w}^T \boldsymbol{K_m} \boldsymbol{a_s} \boldsymbol{B_p} dx \\ \boldsymbol{K_{ww}} &= \int_{l_e} \boldsymbol{B_w}^T \boldsymbol{a_w}^T \boldsymbol{K_m} \boldsymbol{a_w} \boldsymbol{B_w} dx \end{aligned} \quad \boldsymbol{P_e} = \begin{bmatrix} \int_{l_e} \boldsymbol{B_p}^T \boldsymbol{a_s}^T \hat{\boldsymbol{\sigma}}(\epsilon^P, \epsilon^w) dx \\ \int_{l_e} \boldsymbol{B_w}^T \boldsymbol{a_w}^T \hat{\boldsymbol{\sigma}}(\epsilon^P, \epsilon^w) dx \end{bmatrix} \tag{10}$$

IMPLEMENTATION OF LONGITUDINAL AND TRANSVERSAL REBARS

In the case of reinforced concrete elements, the contribution of the longitudinal rebars must be added to that of the concrete fibers. The total section will thus be represented by the sum of the concrete area and the section of the longitudinal reinforcement. The latter one is modeled as point elements intersecting the concrete cross-section. The shape and dimensions of the bar are considered as negligible. Consequently, the warping and distortion of this point element are not taken into account. It follows that the deformations of these elements are composed only by the terms of the plane strain field $\boldsymbol{\varepsilon}^{\mathbf{P}}$ defined by Timoshenko's theory. Regarding the implementation of stirrups, they are modeled as bar elements with linear elastic constitutive law. Each leg of the transversal rebars is discretized into n_{st} sub-elements of length l_{st}, presenting two nodes where the transversal distortional displacements components $\mathbf{u_{wy}}$ and $\mathbf{u_{wz}}$ are computed as presented by Figure 3.

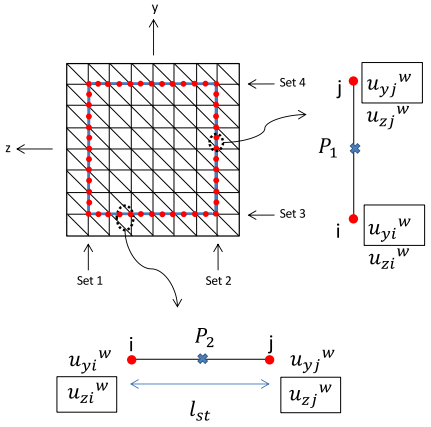

Figure 3: Cross-section discretization: concrete and transversal steel reinforcement mesh

Linear Lagrange polynomials are used to interpolate distortion between these two nodes at a single integration Gauss point P. All transversal sub-element rebars colinear to y-direction belong to (Set 1) or (Set 2), whereas those towards z-direction are attributed to (Set 3) and (Set 4) as seen in Figure 3. Having the expression of the displacement at points P1 and P2, the enhanced transversal strain can be deduced. On the other hand, the contribution of the transversal rebars can be seen at the sectional level, with extra terms added to $\mathbf{P_s}$ and $\mathbf{K_s}$ such that:

$$\boldsymbol{K_s} = \begin{bmatrix} \boldsymbol{K_{spp,c}} & \boldsymbol{K_{spw,c}} \\ \boldsymbol{K_{swp,c}} & \boldsymbol{K_{sww,c}} + \boldsymbol{K_{sww,st}} \end{bmatrix} \tag{11}$$

VALIDATION PROCESS: NUMERICAL CASE STUDIES

All the simulations in this paper have been performed on the platform ATL4S developed at INSA Lyon [10] for internal numerical developments and initially inspired by the philosophy of FEDEASLAB for data entry [11].

Concrete beam element confined with stirrups

This section highlights the role of stirrups on confining concrete fibers. To this end, dilation effect is simulated by imposing a thermal dilation effect to the concrete fibers in the linear elastic phase. By applying this method and with a large section of stirrups confining the concrete fibers, the initial and deformed shapes of the cross-section are presented in Figure 4 (a,b). Also, it can be seen in Figure 4 (c,d) that the comparison between the proposed multifiber model and the 3D FE model presents a reasonable agreement in terms of transversal displacement maps.

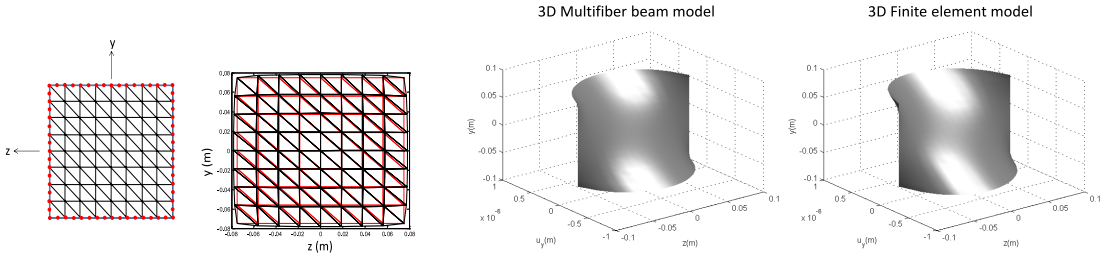

Figure 4: Concrete section confined with stirrups (a). Initial (red) and deformed (black) shape of the cross-section (b) and (c) Transversal displacement maps for concrete fibers confined by large section of stirrups

Compression test on the beam in the non linear domain

The non-linear behaviour of the beam is tested by means of a numerical experiment by comparing the response of the beam with a non-linear damage law (the Mu model [12]) confined by reinforcements in a homogeneous and uniform stress state framework and the direct association of the spring-loaded damage model as a reference example (see also [13]). The detail of the comparison is given by the figure 5 and in [13].

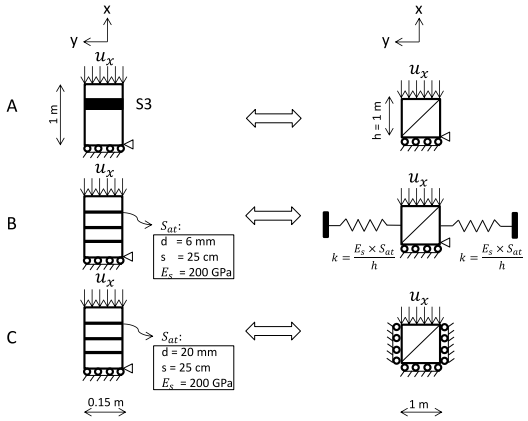

Figure 5. Two-dimensional multifibre beam model (left) and two-dimensional Finite element (right) columns subjected to axial compression: (A) concrete beam without stirrups, (B) concrete beam with moderated amount of stirrups and (C) concrete beam highly confined with transversal rebars.

The comparison between the enhancer multifiber beam element with the 2D model of the confined constitutive law is given in figure 6 for different values of transversal steel area: from 0 stirrups to an important confinement. The simulation with an important quantity of stirrups tends naturally to the case with fixed lateral displacements.

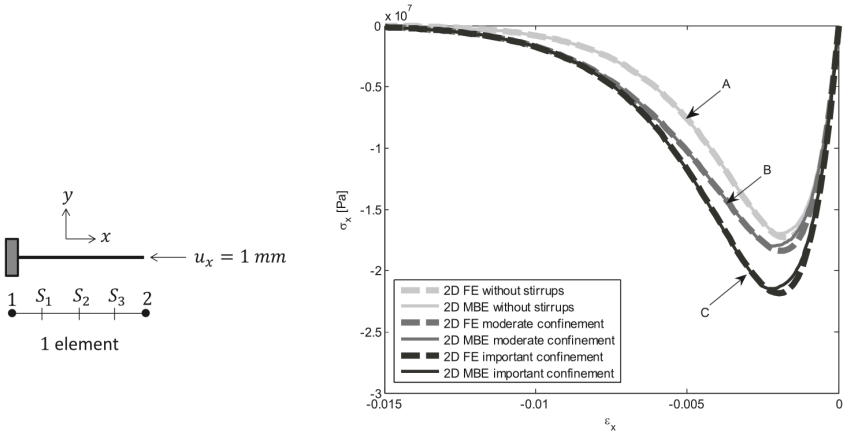

Figure 6. Stress strain compression curve. Comparison between the new enhanced multifiber beam element (section S3) and a 2D representation using finite element method : (A) non confined, (B) concrete confined with a moderate quantity of stirrups (C) concrete confined with an important quantity of transversal stirrups

Compression/bending test compared to experimental results

In order to show the effects of the confinement due to stirrups and the dilatancy effect of the concrete, a numerical analysis using the new beam element is fitted on experimental data. Then the effect of the confinement and the dilatancy are respectively removed in order to show the effect of both of them.

To do so, a 2m high reinforced concrete column tested at the University of Sherbrooke ([14-15]) has been subjected to lateral displacement δ in addition to an axial loading P. The horizontal load during the tests was applied by two jacks with a maximum load of 100 kN. On the other hand, the axial load level applied was the one commonly used in structures, i.e. 15 to 40% of the cross section resistance. Then the column was subjected to a compression load P of about 2900 kN. Figure 3 provides a general description of the investigated column and its reinforcement details.

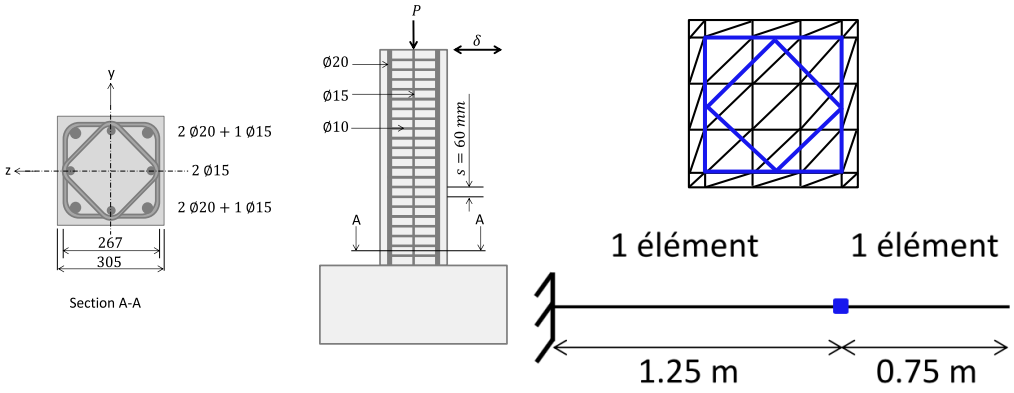

(a) (b) (c)

Figure 7. Reinforced concrete cross section confined with stirrups, (b) columns submitted to axial loading and transversal cyclic displacement [15], (c) Transversal and longitudinal numerical discretization of the column

Since no regularization technique has been adopted in this work, the size of the first beam element, and consequently the distance between two consecutive sections, is based on the size of the plastic hinge that can be determined experimentally. Consequently, the column is discretized longitudinally using 2 enhanced beam elements (with 3 sections per element) as shown in Figure 7 (c). The Menegoto Pinto model [16] has been used for steel using the yield strength of the transverse reinforcement f_{yh}, the longitudinal reinforcement f_y and the corresponding Young's modulus E_s provided in [15].

The other parameters are the fretting spacing s and the diameter φ of the steel bars that can be used directly in the numerical model.

The Mu model has been used to reproduce the behavior of concrete. This model is very suitable in order to reproduce cyclic loading of concrete. However it does not display any dilatancy behavior. In order to address in a simple way this issue, a correction of the Poisson coefficient is proposed by equation 12 in order to generate artificially dilatancy in the concrete, which will generate automatically a confinement effect due to the stirrups. D is the damage variable of the model and starts from 0 for a non-damaged state to 1 for a fully damaged material. This initial Poisson coefficient is taken equal to 0.2.

$$\boldsymbol{\nu = \nu_{initial}(1 + D)} \qquad \textbf{(12)}$$

Table 1 summarizes all concrete characteristics used in the model.

Table 1. Material parameters of the Mu mode used for concrete

E (GPa)	A_t	B_t	A_c	B_c	ϵ_{t_0}(Pa)	ϵ_{c_0} (Pa)
35	0,8	8000	0,7	350	3.10^6	-30.10^6

Figures 8 (A, B and C) show the evolution of the transverse force developed at the top of the column as a function of the imposed transverse displacement δ. Case A shows the inability of the model to reproduce the non-linear behaviour of the column without the introduction of transverse reinforcement. Once these reinforcements are introduced into the numerical model, the strength of the concrete increases (the value of the ultimate force increases) but this is not sufficient to reproduce all the cyclic response. For this reason, and in order to make the concrete more ductile, the expansion is added directly into the Poisson's coefficient according to the method detailed above. By combining the presence of transverse steels with the expansion effect introduced in the constitutive law attributed to the concrete fibre, the non-linear response of the column can be better reproduced.

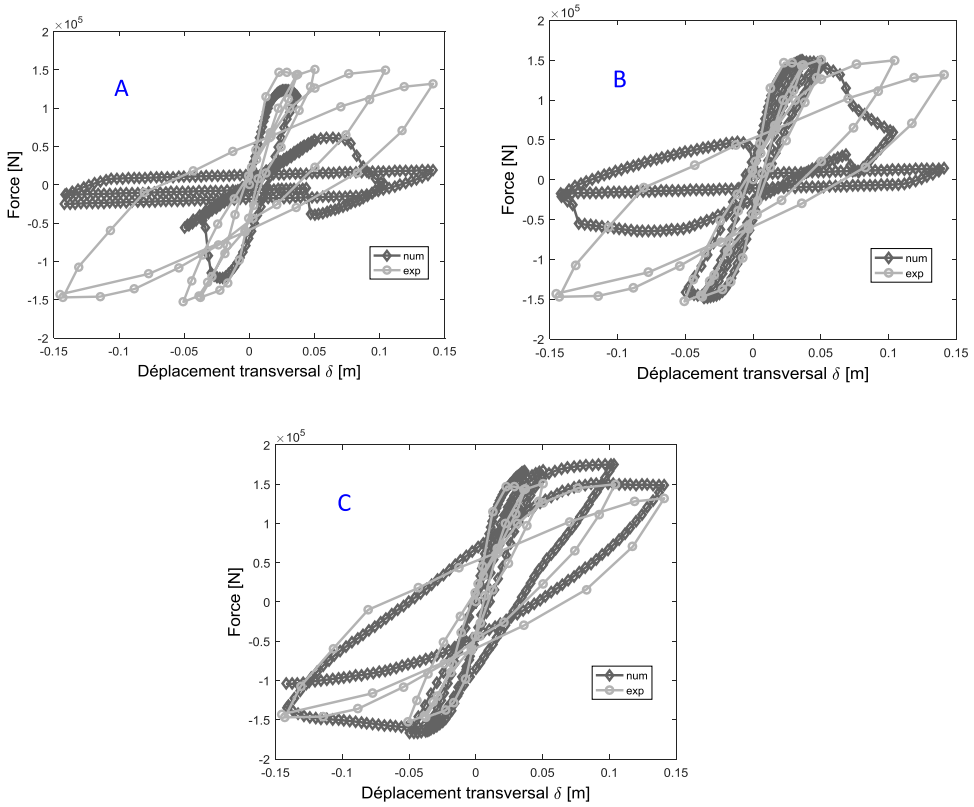

Figure 8. Cyclic tests for the rectangular cross-section column tested at Sherbrooke University C80B60N40 : force-transversal displacement δ relationship, A : without stirrups and whitout additional dilatancy in concrete, B : with stirrups and without additional dilatancy, C : with stirrups and with additional dilatancy in concrete constitutive law.

CONCLUSION

An efficient 3D multifiber beam model was presented aiming at reproducing the vertical stretching of the concrete cross-section confined by stirrups. This distortional effect is taken into account by adding new degrees of freedom to the global level. A novel Timoshenko beam element recently developed by [8] for 2D applications, has been chosen and extended in our model to the 3D formulation in order to avoid shear locking problems. Also, it should be mentioned that the present formulation of the section equilibrium is derived from the one presented by [2], then [4] for reinforced concrete which takes into account the warping of the cross-section. The presented model is suitable for an arbitrary cross-section and material. Its efficiency is highlighted by comparing the numerically obtained results in terms of stresses and displacement with those coming from numerical or experimental tests. Good matching was observed showing the robustness of the enhanced model and validating its performance in the non linear domain. Furthermore, longitudinal and transversal rebars are modelled. Their implementation was validated by introducing a dilatancy effect to the concrete fibers and confronting the obtained outcomes with those coming from a 3D FE model. The case studies investigated herein are related to cyclic loadings using an updating procedure of the Poisson ratio, aiming at reproducing the dilatancy effect due to the presence of stirrups. A nonlinear dilatant constitutive law would have to be implemented and tested on reinforced concrete elements under monotonic and cyclic loadings to reproduce the nonlinear response of structural concrete elements subjected to transverse shear. Also, the mass matrix can be implemented in order to conduct dynamic simulation studies, and the warping effect, taken into account by [4], can be coupled with the distortion of the section in order to obtain a complete 3D enhanced multifiber beam model.

REFERENCES

[1] Guedes, J., P. Pegon, & A. Pinto (1994). A fibre/timoshenko beam element in castem 2000. Applied Mechanics Unit, Safety Technology Institute, Joint Research Center, European Commision, I-21020 Ispra (VA) Italy, Special Publication Nr. I.94.31.

[2] Le Corvec, V. (2012). Nonlinear 3d frame element with multi-axial coupling under consideration of local effects. Ph. D.thesis, University of California, Berkeley.

[3] Mohr, S., J. Bairan, & A. Mar (2010). A frame element model for the analysis of reinforced concrete structures under shear and bending. Engineering structures 32, 3936–3954.

[4] Capdevielle, S., S. Grange, F. Dufour, & C. Desprez (2016). A multifiber beam model coupling torsional warping and damage for reinforced concrete structures. European Journal of Environmental and Civil Engineering 20, 914–935.

[5] Cusson, D. & P. Paultre (1995). Stress-Strain model for con- fined high-strength concrete. Journal of Structural Engineering 121, 468–477.

[6] Ibrahimbergovic, A. & F. Frey (1993). Finite element analysis of linear and non-linear planar deformations of elastic initially curved beams. International Journal for Numerical Methods in Engineering 36, 3239–3258.

[7] Stolarski, H. & T. Belytschko (1982). Membrane locking and reduced integration for curved elements. Journal of Applied Mechanics 49, 172–176

[8] Caillerie, D., P. Kotronis, & R. Cybulski (2015). A timoshenko finite element straight beam with internal degrees of freedom. International Journal For Numerical And Analytical Methods In Geomechanics 39, 1753–1773.

[9] Bitar I. (2017), Modélisation de la rupture dans les structures en béton armé par des éléments finis poutres généralisées et multifibres, PhD thesis, Ecole Centrale de Nantes.

[10] Grange S., 2015. ATL4S - A Tool and Language for Simplified Structural Solution Strategy - Intern. report, GEOMAS.

[11] Filippou, F. C. and M. Constantinides (2004). "FEDEASLab getting started guide and simulation examples." NEESgrid Report 22: 2004-2005.

[12] Mazars J., Hamon F., Grange S., 2015, A new 3D damage model for concrete under monotonic, cyclic and dynamic loading, Materials and Structures, 48, 3779–3793

[13] Khoder N., Grange S., & Sieffert Y. (2018): Enhancement of a two-dimensional multifibre beam element in the case of reinforced concrete structures for taking into account the lateral confinement of concrete due to stirrups, European Journal of Environmental and Civil Engineering, DOI: 10.1080/19648189.2018.1446364

[14] Cardona Jaramillo L. I., Le logiciel BPiCoS dans un contexte de dimensionnement basé sur la performance (DBP), PhD thesis, Université de Sherbrooke, 2008.

[15] Legeron F., Paultre P., Comportement en flexion composée de poteaux en béton à haute performance, BLPC - Bulletin des Laboratoires des Ponts et Chaussées , 202 , Laboratoire Central des Ponts et Chaussées - LCPC, 37–50, 1996.

[16] Menegotto M. Pinto P. E., (1973) Method of analysis for cyclically loaded reinforced concrete plane frames including changes in geometry and non-elastic behavior of elements under combined normal force and bending, IABSE Symposium of Resistance and Ultimate Deformability of Structures Acted on by Well-Defined Repeated Loads, International Association of Bridge and Structural Engineering, Lisbon, Portugal, 13, 15–22.